Vortex Model Based Adaptive Flight Control Using Synthetic Jets

Jonathan Muse, Andrew Tchieu, Ali Kutay, Rajeev Chandramohan, Anthony Calise, and Anthony Leonard

Department of Aerospace Engineering
Georgia Institute of Technology

August 20, 2008

Overview

1. Introduction
2. Experiment Hardware
   - Wind Tunnel Traverse
   - Wing and Actuators
3. Nominal Control Design
   - Actuation Modeled as a Static Device
   - Nonlinear Vortex Model
   - "Linear" Vortex Model
   - Coupled Vortex/Rigid Body Model
   - Nominal Control Designs
4. Adaptive Control Design
   - Plant Dynamics/Reference Behavior
   - Adaptive Control Implementation
   - Saturation Protection
5. Experimental Results
   - Determining Model Parameters
   - Model Validation
   - Closed Loop Experiments

Outline

1. Introduction
2. Experiment Hardware
   - Wind Tunnel Traverse
   - Wing and Actuators
3. Nominal Control Design
   - Actuation Modeled as a Static Device
   - Nonlinear Vortex Model
   - "Linear" Vortex Model
   - Coupled Vortex/Rigid Body Model
   - Nominal Control Designs
4. Adaptive Control Design
   - Plant Dynamics/Reference Behavior
   - Adaptive Control Implementation
   - Saturation Protection
5. Experimental Results
   - Determining Model Parameters
   - Model Validation
   - Closed Loop Experiments

Introduction

- Aerodynamic flow control.
- Enable highly-maneuverable flight for small UAVs (e.g., in confined spaces).
  - No moving control surfaces.
  - Maneuver on convective time scale (Dragon Eye scales: 20 m/s, c 30cm, $t_{conv} = 15\ msec$)
- Flight dynamics and flow dynamics are coupled.
  - Flow develops forces and moments on convective time scales.
  - Flow state is affected by both vehicle dynamics and actuation.

Outline

1. Introduction
2. Experiment Hardware
   - Wind Tunnel Traverse
   - Wing and Actuators
3. Nominal Control Design
   - Actuation Modeled as a Static Device
   - Nonlinear Vortex Model
   - "Linear" Vortex Model
   - Coupled Vortex/Rigid Body Model
   - Nominal Control Designs
4. Adaptive Control Design
   - Plant Dynamics/Reference Behavior
   - Adaptive Control Implementation
   - Saturation Protection
5. Experimental Results
   - Determining Model Parameters
   - Model Validation
   - Closed Loop Experiments

Experiment Diagram

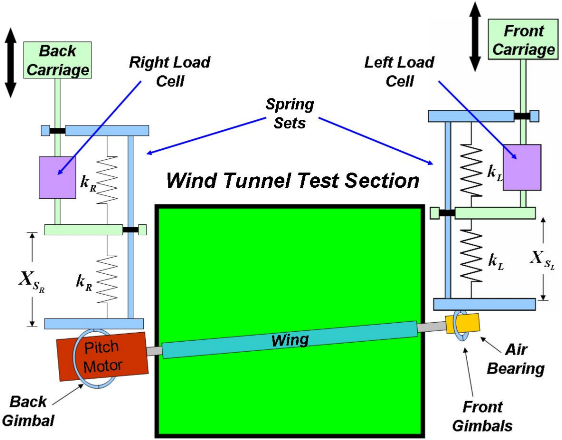

Traverse

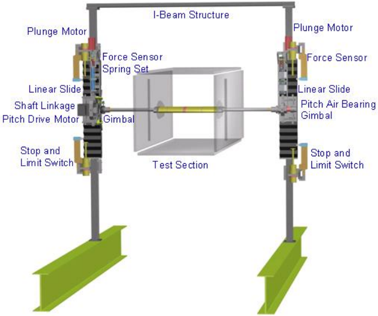
I-Beam Structure
Plunge Motor
Plunge Motor
Force Sensor
Spring Set
Force Sensor
Linear Slide
Linear Slide
Shaft Linkage
Pitch Air Bearing
Gimbal
Pitch Drive Motor
Gimbal
Stop and
Limit Switch
Stop and
Limit Switch
Test Section

Force Control

- **Purpose:** Simulation of longitudinal free flight in a wind tunnel.
- A force control technique was developed to accomplish this.
- Force control maintains prescribed force/moment on model.
    - Removes effect of gravity.
    - Hides traverse nonlinearities from model.
    - Applies prescribed force commands to the traverse.
    - Feedback of wing states alters dynamics of flying model.
- Force is applied by regulating the deflection of the springs in the traverse.
- Moment applied via torque motor.

Traverse Mechanism

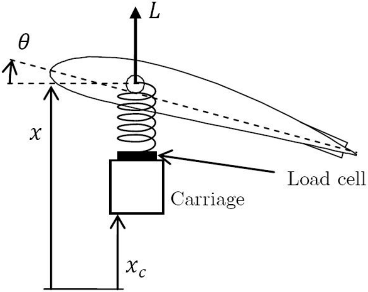

- Inner loop PID control laws regulate the carriage positions.
- Force control law commands accelerations to the carriages.
- Allows regulation of the spring deflection on the airfoil.

Wing Model

- 1m span NACA 4415 wing section
- Chord length is 457 mm.
- Modular and comprised of interchangeable spanwise segments for sensors.
- Includes module of a circumferential array of 70 static pressure ports located at mid-span.
- Several modules of high-frequency integrated pressure sensors for measurements of instantaneous pressure.

Wing Section

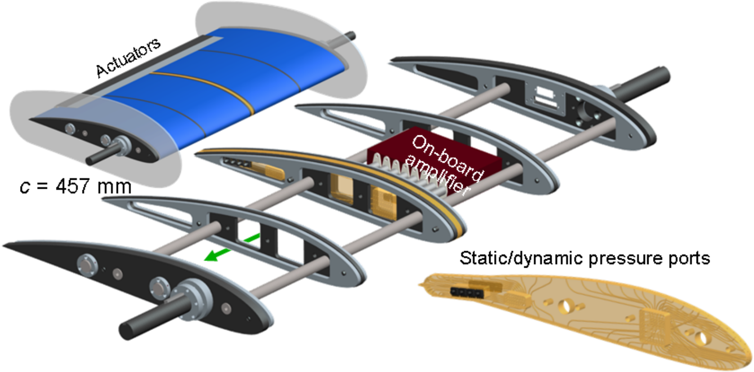

Flow Control Actuators

- Synthetic jet type actuators.
- Array of jets mounted on trailing edge of wing.
- Actuators are amplitude modulated.

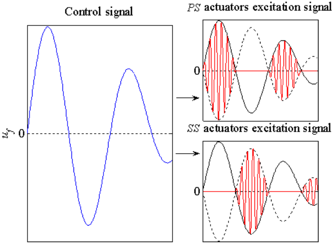

- Characteristic actuation rise time O(2-3tconv).
- Usable control authority up to 30 Hz in pitch.

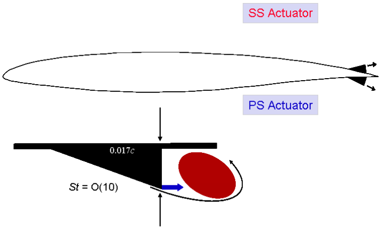

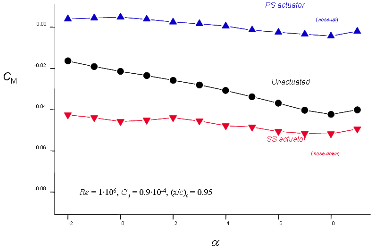

- Hybrid actuators on opposite sides of the trailing edge allow CM to be varied bidirectionally without moving surfaces.
  - Manipulates concentrations of trapped vorticity.
  - PS actuator increases C_M (nose-up).
  - SS actuator decreases C_M (nose-down).
- Significant changes in C_M with minimal lift and drag penalty
- Changes in actuator C_μ allow aerodynamic performance to be continuously varied

System, Concept

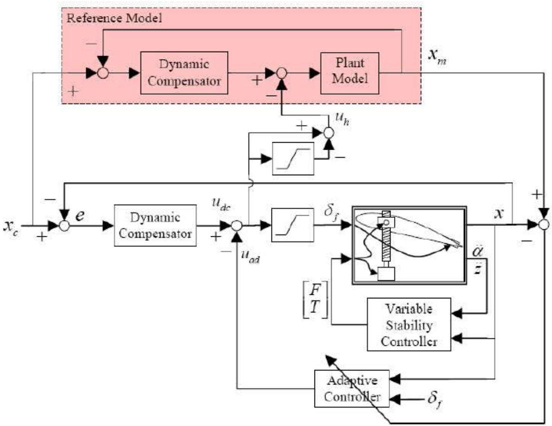

Outline

1. Introduction
2. Experiment Hardware
   - Wind Tunnel Traverse
   - Wing and Actuators
3. Nominal Control Design
   - Actuation Modeled as a Static Device
   - Nonlinear Vortex Model
   - "Linear" Vortex Model
   - Coupled Vortex/Rigid Body Model
   - Nominal Control Designs
4. Adaptive Control Design
   - Plant Dynamics/Reference Behavior
   - Adaptive Control Implementation
   - Saturation Protection
5. Experimental Results
   - Determining Model Parameters
   - Model Validation
   - Closed Loop Experiments

Static Actuator Model of the Wing

- The effect of an actuator is modeled as a static moment actuator.
- The lift and moment can be modeled as

$$L = QS\left(C_{L_0} + C_{L_\alpha}\alpha + C_{L_{\dot{\alpha}}}\dot{\alpha}\right)$$

$$M = QS\bar{c}\left(C_{M_0} + C_{M_\alpha}\alpha + \frac{\bar{c}}{2V_\infty}C_{M_{\dot{\alpha}}}\dot{\alpha} + C_{M_{\delta_a}}\delta_a\right)$$

- Modeling leads to a system model of the form

$$\begin{bmatrix} \dot{y} \\ \ddot{y} \\ \dot{\alpha} \\ \ddot{\alpha} \end{bmatrix} = \begin{bmatrix} 0 & 1 & 0 & 0 \\ 0 & a_{2,2} & a_{2,3} & a_{2,4} \\ 0 & 0 & 0 & 1 \\ 0 & a_{4,2} & a_{4,3} & a_{4,4} \end{bmatrix} \begin{bmatrix} y \\ \dot{y} \\ \alpha \\ \dot{\alpha} \end{bmatrix} + \begin{bmatrix} 0 \\ 0 \\ 0 \\ b_{f,4} \end{bmatrix} \delta_a$$

Concept of Vortex Model

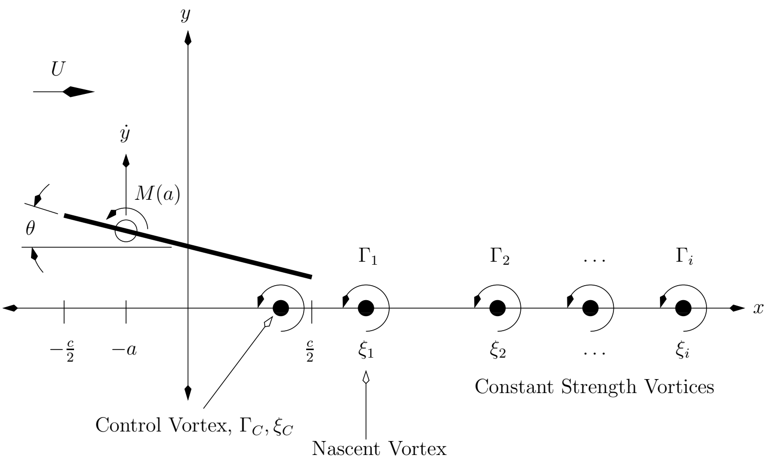

Nonlinear Vortex Model

- From our previous work, we obtained the following lift and moment relations

$$L = -\rho\pi(\tfrac{c^2}{4}\ddot{y} + Uc\dot{y}) + \rho\pi\left[\frac{ac^2}{4}\ddot{\theta} + U(a+\tfrac{c}{2})c\dot{\theta} + (\frac{\dot{U}c^2}{4} + U^2c)\theta\right]$$
$$-\frac{\rho Uc}{2}\sum_{i=1}^{N}\frac{\Gamma_i}{\sqrt{\xi_i^2 - c^2/4}} + \rho U\Gamma_C$$

and

$$M(a) = aL + \frac{\rho\pi Uc^2}{4}\dot{y} + \rho\pi\left[\frac{c^4}{128}\ddot{\theta} - \frac{Uac^2}{4}\dot{\theta} - \frac{U^2c^2}{4}\theta\right]$$
$$+\frac{\rho Uc^2}{8}\sum_{i=1}^{N}\frac{\Gamma_i}{\sqrt{\xi_i^2 - c^2/4}} + \rho U\Gamma_C\xi_C$$

Nonlinear Vortex Model

- The shed vortex positions, ξ_i, were given by

$$\frac{d\xi_1}{dt} = U - \frac{(\xi_1^2 - c^2/4)}{\xi_1 \Gamma_1} \frac{d\Gamma_1}{dt}$$
$$\frac{d\xi_i}{dt} = U \quad (i \geq 2)$$

- The vortex strengths, Γ_i, were defined by

$$\Gamma_1 = -\sqrt{\frac{\xi_1 - c/2}{\xi_1 + c/2}} \left(\Gamma_0 + \sum_{i=2}^{N} \sqrt{\frac{\xi_i + c/2}{\xi_i - c/2}} \right)$$
$$\Gamma_i = Constant$$

Corrections for Thickness and Camber

- Corrections needed for accurate simulation.
- Corrections based on NASA legacy data.
- Effect of thickness and camber is to translate lift and moment curves.
- Lift changes as

$$\tilde{L} = L + \left(\frac{1}{2}\rho U^2 c\right) C_{L,0}$$

- Moment changes as

$$\tilde{M} = M - \left(\frac{1}{2}\rho U^2 c^2\right) C_{M,0} + \left(a - \frac{c}{4}\right)\left(\frac{1}{2}\rho U^2 c\right) C_{L,0}$$

- In our experiments, the c.g. is close to quarter chord and M simplifies since $\left(a - \frac{c}{4}\right) \approx 0$

Linear Model Development

- Vortex model captures dynamics that are negligible on time scales of rigid body dynamics.
- We define a characteristic circulation as

$$\Gamma_W = c \sum_{i=1}^{N} \frac{\Gamma_i}{\sqrt{\xi_i^2 - c^2/4}}$$

- We consider the lift and moment generated when impulsively started from rest
  - $d\Gamma_w/dt = 0$.
  - Only a single vortex is created.

Linear Model Development (cont.)

- This gives the lift as

$$L = -\rho U \left(\Gamma_0 - \frac{1}{2} \Gamma_W \right)$$

- At $t = t_0$, $\Gamma_W \approx -\Gamma_0$.
- When $t \to \infty$, Lift terms should disappear as wake vortices move downstream.
- To model as linear, we propose the following model

$$\frac{d\Gamma_W}{dt} = -\frac{d\Gamma_0}{dt} - \beta \Gamma_W$$

where β is a constant and the initial condition of the differential is

$$\Gamma_W(t_0) = \Gamma_0(t_0)$$

The Linear Model

- This induces an exponential rise in lift $(1 - e^{\beta t})$ for a constant Γ_0.
    - This is contrary to the classical square root type growth for lift.
    - This is contrary to the decay in lift that is geometric at best.
- One can compute the best fit for β at a given Δt.
- Hence, the "linearized" characteristic circulation is

$$\dot{\Gamma}_W + \beta\Gamma_W = -\pi c\left(\ddot{y} + \left(a + \frac{c}{4}\right)\ddot{\theta} + U\dot{\theta}\right)$$

with an initial condition of

$$\Gamma_W(t_0) = -\pi c\left(\ddot{y} + \left(a + \frac{c}{4}\right)\ddot{\theta} + U\dot{\theta}\right)\Bigg|_{t=t_0}$$

Linear Lift/Moment Relationships

- The lift and moment expressions simplify to:

$$L = -\rho\pi\left(\frac{c^2}{4}\ddot{y} + Uc\dot{y}\right) - \rho U\left(\frac{1}{2}\Gamma_W + \Gamma_C\right)$$
$$- \rho\pi\left[\frac{ac^2}{4}\ddot{\theta} + U\left(a + \frac{c}{2}\right)c\dot{\theta} + \left(\frac{\dot{U}c^2}{4} + U^2 c\right)\theta\right]$$

and

$$M = aL + \frac{\rho\pi Uc^2}{4}\dot{y} + \rho\pi\left[\frac{Uac^2}{4}\dot{\theta} + \frac{U^2c^2}{4}\theta - \frac{ac^2}{128}\ddot{\theta}\right]$$
$$+ \rho U\left(\frac{c}{8}\Gamma_W - \Gamma_C\xi_C\right)$$

The above equations include added mass, quasi-steady lift, lift due to wake, and control terms.

Coupled Model Assumptions

- Assume the rigid body dynamics are given by

$$\begin{aligned} m\ddot{y} + b_y\dot{y} + k_y y &= L \\ I\ddot{\theta} + b_\theta\dot{\theta} + k_\theta\theta &= M(a) \end{aligned}$$

- L is the lift.
- $M(a)$ is the moment about the location a.

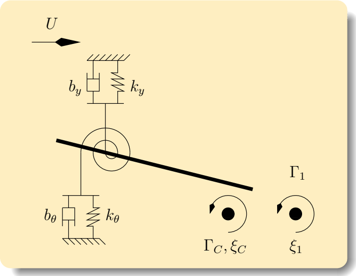

- Neglect thickness and camber corrections for control design purposes.

Redefining Lift and Moment as Matrix Equations

- The "Linear" Vortex Model can be written as

$$\dot{x} = Ax + B\Gamma_C$$

where $x = [y \quad \theta \quad \dot{y} \quad \dot{\theta} \quad \Gamma_w]^T$.

- How does Γ_C relate to the physical world?
- Γ_C can be related to applied moment as

$$\Gamma_C(u_f, \theta) = \frac{1}{2} Uc \left(\frac{a + \xi_C}{c} \right) \Delta C_M(u_f, \theta)$$

- $C_M(u_f, \theta)$ is determined from static experimental data.
- Hence, the model becomes nonlinear!
- Luckily, $\Gamma_C(u_f, \theta)$ is invertible for fixed θ.

Nominal Control Designs

- The vortex model is nonlinear.
- $\Gamma_C(u_f, \theta)$ is invertible for fixed θ
- We employ an inversion technique to make the control design effectively linear.

$$\xrightarrow{\Gamma_C} \boxed{\Gamma_C^{-1}(\cdot,\theta)} \xrightarrow{u} \boxed{\dot{x} = \bar{A}x + \bar{B}\Gamma_C(\cdot,\theta)} \xrightarrow{x}$$

- Inversion of $\Gamma_C(u_f, \theta)$ is pre-computed in a lookup table.
- Now, one can use standard linear analysis tools to develop control laws based on the static actuator model and the vortex model.

Linear Control Law Design

- Defining the tracking error

$$e = y - r$$

- We must design a control law to ensure

$$e(t) \rightarrow 0 \; as \; t \rightarrow \infty$$

- Using a modified robust servomechanism LQR like formulation, feedback gains, K_e and K_x, are computed.
- Results in a control law of the form

$$u = -K_e \int_0^t e(\tau) d\tau - K_x x + Zr$$

Nominal Control Architecture

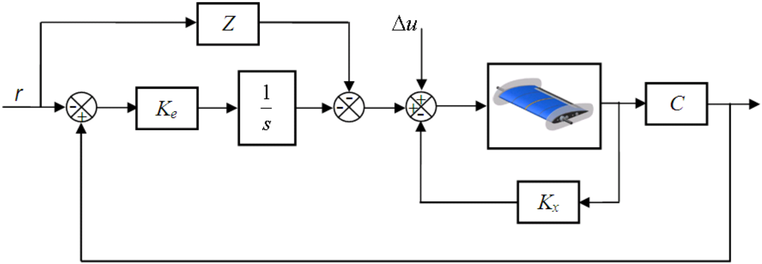

Robust Servo LQR with feedforward element

Avoiding State Estimation for Vortex Control Law

- State feedback is not possible for vortex model.
- Aerodynamic state is unmeasurable.
- We modify the nominal vortex design using projective control.
- Augmenting the model dynamics with the control law dynamics, the closed loop system is given by

$$\begin{bmatrix} e \\ \dot{x} \end{bmatrix} = \begin{bmatrix} 0 & C \\ -\bar{B}K_e & \bar{A} - \bar{B}K_X \end{bmatrix} \begin{bmatrix} \int e \\ x \end{bmatrix} + \begin{bmatrix} -1 \\ \bar{B}Z \end{bmatrix} r$$

$$y = \begin{bmatrix} 0 & C \end{bmatrix} \begin{bmatrix} e \\ x \end{bmatrix}$$

where C is a matrix that multiplied by x gives the position.

Avoiding State Estimation for Vortex Control Law

- We can retain all but one of the closed loop eigenvalues.
- Let $K = [K_e \quad K_x]$ and X_y be the eigenvectors corresponding to the closed loop eigenvalues we wish to retain.
- The required output feedback gain is given by

$$\bar{K} = K X_y \left(\bar{C}_{measured} X_y \right)^{-1}$$

where $\bar{C}_{measured}$ corresponds to the rigid body states of x.

New Output Feedback Vortex Control Law

$$u = -K \begin{bmatrix} \int e \\ y_{measured} \end{bmatrix} + Zr$$

Outline

1. Introduction
2. Experiment Hardware
   - Wind Tunnel Traverse
   - Wing and Actuators
3. Nominal Control Design
   - Actuation Modeled as a Static Device
   - Nonlinear Vortex Model
   - "Linear" Vortex Model
   - Coupled Vortex/Rigid Body Model
   - Nominal Control Designs
4. Adaptive Control Design
   - Plant Dynamics/Reference Behavior
   - Adaptive Control Implementation
   - Saturation Protection
5. Experimental Results
   - Determining Model Parameters
   - Model Validation
   - Closed Loop Experiments

Plant Dynamics/Reference Behavior

- We assume that our plant can be expressed as

$$\dot{x}(t) = Ax(t) + B\Lambda\left[\Gamma_C(t) + f(x, \Gamma_C)\right]$$
$$y(t) = Cx(t)$$

- The nominal control law can be expressed as

$$\Gamma_{C,n} = -K_y y + K_r r$$

- Assuming $f(x, \Gamma_C) = 0$, we form the desired behavior

$$\dot{x}_m(t) = A_m x_m(t) + B_m r$$
$$y_m(t) = Cx_m(t)$$

where $A_m = A - BK_r$ is Hurwitz and $B_m = BK_r$.

Approximating System Uncertainty

- We want to design an adaptive signal $\Gamma_{C,ad}$ to approximately cancel the modeling error $f(x, \Gamma_C)$.
- The total control effort becomes

$$\Gamma_C(t) = \Gamma_{C,n}(t) - \Gamma_{C,ad}(t)$$

- We will try to approximate $\Lambda f(x, \Gamma_C)$ with a SHL neural network

$$\Lambda f(x, u) = W^T \bar{\sigma}(V^T \eta(t)) + \epsilon(x, u), \quad (x, u) \in \mathcal{D}_x \times \mathcal{D}_u$$

where ϵ, W, and V are unknown but bounded.
- We reconstruct the nonlinearity via delayed values of system outputs and inputs as inputs to the neural network ($\eta(t)$).

Error Observer

- Since all of the states are not observable, we need an error observer.

$$\dot{\xi} = A_m \xi + L(y - y_\xi - y_m)$$
$$y_\xi = C\xi$$

where $\tilde{A} = A_m - LC$ is Hurwitz and satisfies the following Lyapunov equation

$$\tilde{A}^T \tilde{P} + \tilde{P}\tilde{A} = -\tilde{Q}, \quad \tilde{Q} = \tilde{Q}^T > 0, \quad \tilde{Q} \in \mathbb{R}^{nxn}$$

- The observer allows us to estimate the error state, $x_m - x$, of the system.

Adaptive Weight Update Laws

- The adaptive update laws are

$$\dot{\hat{W}}(t) = -\Gamma_W Proj\left[\hat{W}(t), \tilde{\sigma}\left(\hat{V}(t), \eta(t)\right)\xi(t)^T PB\right]$$

$$\dot{\hat{V}}(t) = -\Gamma_V Proj\left[\hat{V}(t), \eta(t)\xi^T PBH\left(\hat{W}(t), \hat{V}(t), \eta(t)\right)\right]$$

$$\dot{\delta\hat{\Lambda}}^T(t) = -\Gamma_\delta Proj\left[\delta\hat{\Lambda}^T(t), u(t)\xi^T(t)PB\right]$$

where

$$\tilde{\sigma}\left(\hat{V}(t), \eta(t)\right) = \bar{\sigma}\left(\hat{V}(t)^T\eta(t)\right) - \bar{\sigma}'\left(\hat{V}(t), \eta(t)\right)\hat{V}^T(t)\eta(t)$$

$$H\left(\hat{W}(t), \hat{V}(t), \eta(t)\right) = \hat{W}^T(t)\bar{\sigma}'\left(\hat{V}(t), \eta(t)\right)$$

- These laws use parameter projection.
- See the paper for additional details.

Compensating for Saturation

- Hedged reference model

$$\dot{x}_m = A_m x_m + B_m r + B_h \Gamma_{C,h}$$

Scheduled Control Hedging

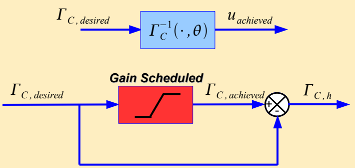

Gain Map for Hedging

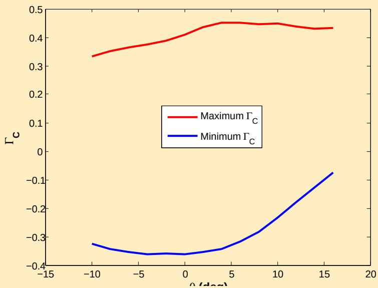

System Conceptual Review

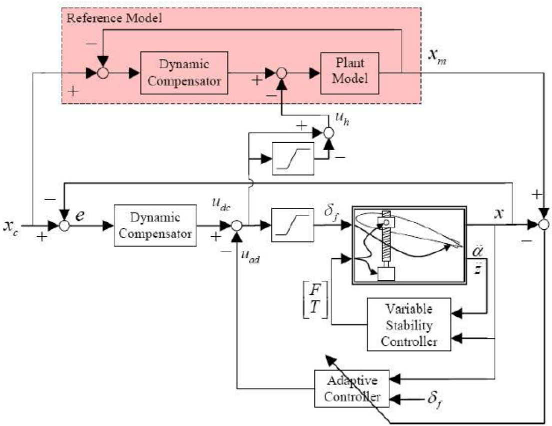

Outline

1. Introduction
2. Experiment Hardware
   - Wind Tunnel Traverse
   - Wing and Actuators
3. Nominal Control Design
   - Actuation Modeled as a Static Device
   - Nonlinear Vortex Model
   - "Linear" Vortex Model
   - Coupled Vortex/Rigid Body Model
   - Nominal Control Designs
4. Adaptive Control Design
   - Plant Dynamics/Reference Behavior
   - Adaptive Control Implementation
   - Saturation Protection
5. Experimental Results
   - Determining Model Parameters
   - Model Validation
   - Closed Loop Experiments

Model Validation

- Static actuator model parameters were determined from static tests.
- Γ_C map was determined from static pitching moment measurements.

Measured $\Gamma_C(u_f, \theta)$

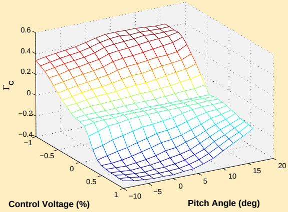

Saturated $\Gamma_C^{-1}(u_f, \theta)$

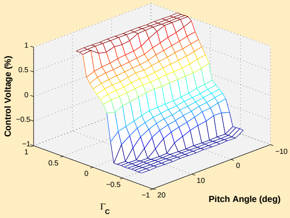

- Saturation of Γ_C ensures invertability.

Model Validation

- Experiment response to open loop actuator excitation has been compared with simulation results.

Flow Control Input Voltage

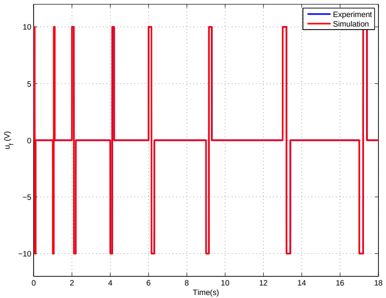

Pitch Response Comparison

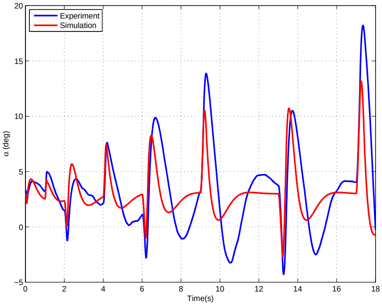

- The vortex ROM performs significantly better than the static actuator model.

Torque Motor Case

- Lets look at the flight response using a torque motor for actuation.

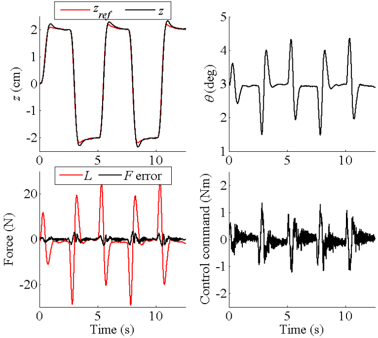

- This indicates that the experiment is closely representing a free flying wing.

Control Law Comparisons

- Square Wave Tracking:

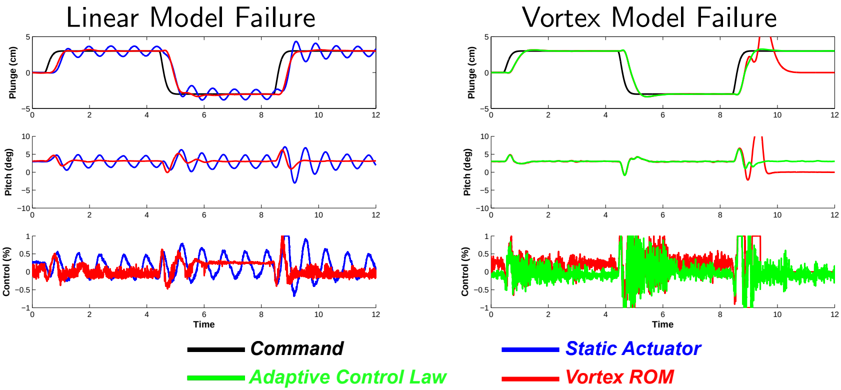

Rise Time Stability Barrier

- Rise time: 10% – 90%
- Static actuator limit: 0.31 *sec*
- Linear vortex model limit: 0.19 *sec*

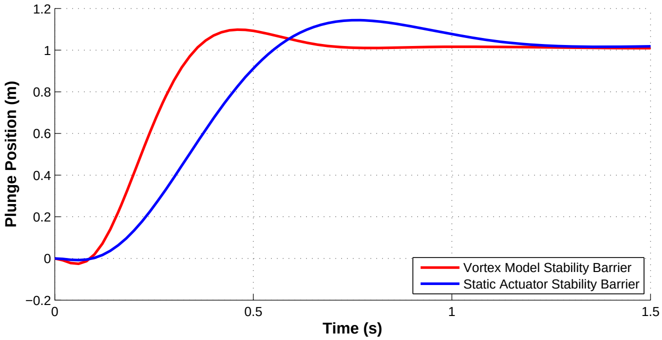

Disturbance Rejection

Conclusions

- Demonstrated closed loop longitudinal control of a wing model using synthetic jet type actuation.
- As the wing moves faster, the actuators can no longer be considered static.
- Simple vortex model developed to allow linear control designs to reach higher bandwidth.
- Unmodeled dynamics destabilize linear control designs at a high enough bandwidth.
- Adaptive control is able to deal with unmodelled dynamics and maintain stability.

Questions?